1   Proposed Journal Section: Neurosystems

2

3   Title: Differences in Anatomical Connections across Distinct Areas in the Rodent Prefrontal Cortex

4

5   Running Title: Anterior-Posterior Organisation of PFC Connections

6

7

8   Authors: Stacey A Bedwell[1], E Ellen Billett[1], Jonathan J Crofts[1], Chris J Tinsley[1]

9

10   Corresponding author: Stacey A. Bedwell - stacey.bedwell@ntu.ac.uk

11

12   Address #1:
13   School of Science and Technology
14   Nottingham Trent University
15   Clifton Lane
16   Nottingham
17   NG11 8NS

18

19

20   **Number of pages: 30**

21   **Number of figures: 10**

22   **Number of tables: 1**

23   **Number of words (abstract): 235**

24   **Number of words (introduction): 573**

25   **Number of words (whole manuscript): 6010**

26

27   Keywords: cortical circuitry, temporal cortex, sensory-motor cortex, organization, tracing.

28

29   Conflicts of Interests:

30   The authors declare no conflict of interests

31

32   Author Contributions:

33

34   SAB performed the anatomical processing and analysed the data. SAB and CJT performed the
35   experiments and wrote the manuscript. EEB, JJC and CJT co-designed the experiments and
36   contributed to the choice of statistical analyses and EEB and JJC edited the manuscript.

37

38

39

40

41

42 **Abstract**

43 Prefrontal cortex (PFC) network structure is implicated in a number of complex higher-order

44 functions and with a range of neurological disorders. It is therefore vital to our understanding of PFC

45 function to gain an understanding of its underlying anatomical connectivity. Here, we injected Fluoro-

46 Gold and Fluoro-Ruby into the same sites throughout rat PFC. Tracer injections were applied to two

47 coronal levels within the PFC (anterior +4.7mm to bregma and posterior +3.7mm to bregma). Within

48 each coronal level, tracers were deposited at sites separated by approximately 1mm and located

49 parallel to the medial and orbital surface of the cortex. We found that both Fluoro-Gold and Fluoro-

50 Ruby injections produced prominent labelling in temporal and sensory-motor cortex. Fluoro-Gold

51 produced retrograde labelling and Fluoro-Ruby largely produced anterograde labelling. Analysis of

52 the location of these connections within temporal and sensory-motor cortex revealed a consistent

53 topology (as the sequence of injections was followed mediolaterally along the orbital surface of each

54 coronal level). At the anterior coronal level, injections produced a similar topology to that seen in

55 central PFC in earlier studies from our laboratory (i.e. comparing equivalently located injections

56 employing the same tracer), this was particularly prominent within temporal cortex. However, at the

57 posterior coronal level this pattern of connections differed significantly, revealing higher levels of

58 reciprocity, in both temporal cortex and sensory-motor cortex. Our findings indicate changes in the

59 relative organization of connections arising from posterior in comparison to anterior regions of PFC,

60 which may provide a basis to determine how complex processes are organized.

61

62

63

Rat prefrontal cortex (PFC) is known to be crucially important in mediating a variety of cognitive (Alvarez and Emory, 2006; Fuster, 2001; Kolb, 1984; Schoenbaum and Roesch, 2005) and autonomic functions (Neafsey, 1990; Frysztak and Neafsey, 1994) yet it's anatomical structure is still not entirely described. In the rat brain prefrontal cortex is divided into distinct cytoarchitectural divisions within a broader grouping of medial and orbital PFC. Medial PFC includes the prelimbic (PL), infralimbic (IL) and anterior cingulate regions (Vertes, 2004; Vertes, 2006). Orbital PFC contains medial orbital (MO), ventral orbital (VO), ventral lateral orbital (VLO) and lateral orbital (LO) regions (Krettek and Price, 1977; Van De Werd and Uylings, 2008). The dorsal lateral orbital region (DLO) lies between LO and the agranular insular area (AI) (Van De Werd and Uylings, 2008). Medial PFC (mPFC) and orbital PFC are proposed to be functionally distinct (Schoenbaum and Roesch, 2005; Schoenbaum and Esber, 2010) and both regions are known to display different connections to other brain sites. Medial PFC is known to play important roles in the timing of motor behaviours (Narayanan and Laubach, 2006; Narayanan and Laubach, 2008; Narayanan and Laubach, 2009; Smith et al., 2010; Kim et al., 2013) and orbital PFC is proposed to provide information in terms of the expected outcomes of events (Schoenbaum and Esber, 2010; Schoenbaum and Roesch, 2005; Stalnaker et al., 2015).

80

Anatomical studies have reported topological projections from PFC to temporal and sensory-motor regions in rats (Sesack et al., 1989; Vertes, 2004; Hoover and Vertes, 2011; Kondo and Witter, 2014; Bedwell et al., 2014; Bedwell et al., 2015). Further topological connections have been reported in the projections from temporal cortex and sensory-motor cortex to PFC (Delatour and Witter, 2002; Bedwell et al., 2014; Bedwell et al., 2015; Reep et al., 1996). Ordering of connections from PFC to subcortical regions have also been described in the connections from PFC to the striatum (Berendse et al., 1992; Schilman et al., 2008). Taken together these studies provide strong evidence for topological PFC connections. Within a wider context of brain connectivity this is entirely consistent

because there is evidence that both sensory-motor cortex (Porter and White, 1983; Aronoff et al., 2010; Henry and Catania, 2006) and temporal cortex (Delatour and Witter, 2002; Arnault and Roger, 1990; Burwell et al., 1995) contain topographically arranged connections to other brain regions.

Typically, the topological ordering of PFC connections has often been described along the medial lateral axis. Changes in the organisation of rat cingulate PFC connections along the anterior-posterior (A-P) axis have also been identified (Olson and Musil, 1992). It is unclear whether or not this is a wider organisational principle also present in other regions, or what the precise functional relevance of such an organisation might be. However, it has been proposed that there are changes in cognitive processing characteristics, such as abstraction in anterior compared to posterior prefrontal cortex in humans (Taren et al., 2011).

The current study aimed to investigate how the organisation of connections changes between anterior and posterior PFC. The neuronal tracers Fluoro-Gold and Fluoro-Ruby were injected into regions of medial and lateral PFC (PL, VO, VLO and DLO, AI). We found that anterior and posterior PFC displayed topological connections to temporal and sensory-motor cortex. Our findings show that the topology observed and the relationship between input and output connections changes between anterior and posterior PFC regions, this was clearest in the connections to temporal cortex.

Experimental Procedures

Data was collected from 18 male CD rats (296-367g, Charles River, UK). Animal procedures were carried out in accordance with the UK Animals scientific procedures act (1986), EU directive 2010/63 and were approved by the Nottingham Trent University Animal Welfare and Ethical Review Body. On receipt the animals were examined for signs of ill-health or injury. The animals were acclimatized for 10 days during which time their health status was assessed. Prior to surgery the animals were

114 housed together in individually ventilated cages (IVC; Techniplast double decker Greenline rat

115 cages). The animals were allowed free access to food and water. Mains drinking water was supplied

116 from polycarbonate bottles attached to the cage. The diet and drinking water were considered not to

117 contain any contaminant at a level that might have affected the purpose or integrity of the study.

118 Bedding was supplied by IPS Product Supplies Ltd in the form of 8/10 corncob. Environmental

119 enrichment was provided in the form of wooden chew blocks and cardboard fun tunnels (Datesand

120 Ltd., Cheshire, UK). Post-surgery the animals were individually or pair housed in the same

121 conditions. The animals were housed in a single air-conditioned room within the Biological support

122 facilities barrier unit, Nottingham Trent University. The rate of air exchange was at least fifteen air

123 changes per hour and the low intensity fluorescent lighting was controlled to give 12 h continuous

124 light and 12 h darkness. The temperature and relative humidity controls were set to achieve target

125 values of $21 \pm 2°C$ and $55 \pm 15\%$ respectively.

126

127 Individual bodyweights were recorded on Day - 10 (prior to the start of dosing) and daily thereafter.

128 All animals were examined for overt signs of ill-health or behavioral change immediately prior to

129 surgery dosing, during surgery and the period following surgery. There were no observed clinical

130 signs/symptoms of toxicity or infection. There was no significant effect on body weight development

131 detected.

132

133 Rats were anaesthetized with isoflurane (Merial, Harlow, UK) and placed in a stereotaxic frame with

134 the incisor bar set so as to achieve a flat skull. Buprenorphine (0.05 mg/kg i.m/s.c) and Meloxicam

135 (up to 1 mg/kg s.c/orally) analgesia were provided peri-operatively and for several days post-

136 operatively. Body temperature was monitored during and immediately after surgery using a rectal

137 thermometer. Craniotomies (<1 mm) were made at predetermined stereotaxic coordinates. Sterile

138 tracer solution was deposited into the PFC via a 0.5 µl neuro-syringe (Hamilton, Germany).

139

Injections of anterograde (10% Fluoro-Ruby in distilled water, Fluorochrome, Denver, Colorado (10 nl/min, 2 min diffusion time)) and retrograde tracer (4% Fluoro-Gold in distilled water, Fluorochrome, Denver, Colorado (100 nl/min, 2 min diffusion time)) were targeted at anterior and posterior PL, VO, VLO or DLO/AI with the intention of revealing the anatomical connections of prefrontal regions. The distance between craniotomy co-ordinates (1 mm) was based on the measured spread of tracers in preliminary and previous studies (<1 mm in diameter). Craniotomies were repeated at 2 anterior-posterior levels (+4.2mm and +3.2mm from Bregma) – see full list of animals and corresponding injection sites in table 1. The medial-lateral co-ordinates and depth of injections below the cortical surface at the anterior and posterior levels are shown in Figure 1. Figure 1 shows that the histological assessed locations of the injections differed slightly from the surgical coordinates, i.e. the anterior and posterior injections were assessed as occurring at +4.7mm and +3.7mm with respect to bregma and following the atlas of Paxinos and Watson, 1998. The coordinates were chosen to avoid the sagittal sinus of the forebrain.

Each rat received injections of Fluoro-Ruby (100nl) and/or Fluoro-Gold (100nl) into various subdivisions of PFC, separated by 1 mm and at an angle of 0 degrees from vertical in the medial-lateral and anterior-posterior axes. Rats received an injection of Fluoro-Gold into one hemisphere and an injection of Fluoro-Ruby into the other hemisphere, to allow accurate identification of the tracers injected. Further dual injections of Fluoro-Gold and Fluoro-Ruby were targeted at anterior and posterior VO and DLO/AI. This was performed to test whether the different projections arising from anterograde or retrograde tracer injections into these regions (and notably to the temporal cortex region), were not due differences in the injections sites of the single tracer injections. Dual injections were made via a first injection of Fluoro-Gold, followed by a second injection of Fluoro-Ruby into the same injection site.

165 Following a survival time of 7–9 days, the rats were deeply anesthetized with pentobarbital (Sigma-

166 Aldrich, UK), and transcardially perfused with phosphate buffered saline (PBS) (pH 7.4) (~200 ml)

167 followed by 4% paraformaldehyde (PFA) (pH 7.4) (~200 ml). The brain was subsequently removed

168 and stored for 24 h in 4% PFA in PBS (pH 7.4), followed by cryoprotection in 30% sucrose in PBS.

169

170 *Anatomical processing*

171

172 For analysis of connections, two series of 40μm coronal sections were taken (2 in 6 sections) on a

173 freezing microtome (CM 1900, Leica, Germany). Sections were mounted onto gelatin coated slides.

174 The first series was cover slipped with Vectashield® mounting medium (with propidium iodide) for

175 fluorescent imaging of Fluoro-Gold (for the injection and projection site). A parallel series of 40μm

176 coronal sections was cover slipped with Vectashield® mounting medium (with DAPI) for fluorescent

177 imaging of Fluoro-Ruby (for the injection and projection site).

178

179 Sections were examined using fluorescent microscopy (Fluoro-Ruby and Fluoro-Gold). Fluorescent

180 photos were captured of the injection sites and the anterograde and retrograde labelling using an

181 Olympus DP-11 system microscope with a x4, x10 and x20 objective lens.

182

183 Immunofluorescent staining of alpha tubulin with fluorescein enabled us to visualize where Fluoro-

184 Ruby labelling occurred in relation to cell bodies, thus establishing the anterograde/retrograde nature

185 of Fluoro-Ruby. Alpha-Tubulin was labelled in several animals R37, R38 and R39. Sections were

186 incubated in an alpha-tubulin monoclonal primary antibody (sc-398103, Santa Cruz, TX) at a dilution

187 of 1:50 overnight at 4ºC and secondary antibody (Fluorescein Horse Anti-Mouse IgG Antibody,

188 Vector Laboratories, UK (in PBS, 2% NS) at a dilution of 1:75 for 1-2 hours. Fluorescein stained

189 sections were cover-slipped with Vectashield® mounting medium (with DAPI) for fluorescent

7

190 imaging. Fluoro-Ruby labels, DAPI stained nuclei and fluorescein stained α-Tubulin were visualized

191 at a high resolution using confocal microscopy.

192

193 *Microscopic analysis*

194

195 The entire forebrain was examined for afferent and efferent connections. Areas of temporal and

196 sensory-motor cortex were found to contain the strongest and most consistent

197 labelling of connections from anterior and posterior PFC. A more detailed analysis was carried out

198 on these regions to examine the organisation of connections across PFC.

199 Alpha-tubulin and Fluoro-Ruby labelling was visualised with confocal microscopy. A Z-series of

200 images was taken at X10, X20 and X40 magnification in sequential scanning mode for each channel

201 using Leica confocal software (LAS AF). Step size between consecutive sections was 1.5μm. In total

202 13 images were taken for each section, across 20.5μm. Each maximal image was composed of

203 multiple sections to ensure optimum capture of the fluorescent tracers/stains.

204

205 ImageJ (Wayne Rasband, NIH) was used to determine numerical values representing the location of

206 retrograde and anterograde labelling in temporal and sensory-motor cortex in 3 dimensional

207 coordinates, x, y and z. The dorsoventral and medial-lateral distance (i.e. laminar location) of each

208 Fluoro-Gold labelled cell in temporal cortex was measured from the rhinal sulcus and cortical surface

209 respectively (in mm). The anterior-posterior location of each retrogradely labelled cell in temporal

210 cortex was also recorded, in terms of distance (mm) from Bregma according to a stereotaxic atlas

211 (Paxinos and Watson, 1998). This process was repeated for Fluoro-Ruby labelling where anterograde

212 axon terminals were usually located close to the cell membrane of neuronal cell soma. A similar

213 acquisition of data was implemented for afferents/efferents in sensory-motor cortex, whereby the

214 dorsoventral and medial-lateral distance of retrograde cells/axon terminals from the cortical surface

215 was recorded (dorsoventral distance was measured from the dorsal aspect of the cortical surface and

216 the medial-lateral measurement was recorded as the distance from the midline). The anterior-posterior

217 location of each retrograde/anterograde marker in sensory-motor cortex was also recorded, in terms

218 of distance (mm) from Bregma. The position of all the individual afferent/efferent labelling associated

219 with an individual tracer injection were recorded and the x, y and z values were calculated as a mean

220 for each injection.

221

222 *Stastistical Analyses*

223

224 Retrograde labelled cells or afferent axon terminal positions were grouped according to injection site

225 location and the positional data was found to be normally distributed. The data sets were analysed

226 with 2 factor ANOVA (injection site, tracer) using SPSS (IBM) to verify the effect of injection

227 location on positioning of labelled cells in anterior-posterior, dorsoventral and medial-lateral

228 dimensions. All statistical tests were applied with a significance level of 0.05 and confidence intervals

229 of 95%.

230 **Results**

231

232 Fluoro-Gold afferents were found in areas of primary and secondary motor cortex (M1, M2), primary

233 somatosensory cortex (jaw region and barrel field - S1J, S1BF), area 1 of cingulate cortex (Cg1),

234 piriform cortex (Pir), perirhinal cortex (PRh - areas 35v, 35d, 36d, 36v), entorhinal cortex (Ent),

235 primary auditory cortex (Au1), ventral secondary auditory cortex (AuV) and prefrontal regions.

236 Fluoro-Ruby labelling was found in areas of M2, S1J, Cg1, S2, PRh, Ent, dorsal agranular insular

237 cortex (AI) and prefrontal regions. The organisation of input and output connections was investigated

238 separately at two anterior-posterior PFC locations (anterior (4.7mm from Bregma) and posterior

239 (3.7mm from Bregma)).

240

Injections into anterior and posterior PFC

Fluoro-Gold injection sites in the anterior (bregma + 4.7mm) and posterior (bregma +3.7mm) aspect of PFC were observed in PL, VO, VLO and DLO anteriorly, and in PL, Cg1, IL, MO,VO, VLO, LO, AI, Dysgranular insular areas (DI) and Granular Insular cortex (GI) posteriorly (Figure 1ii, iv). These injection sites were mostly confined to layers I-V/VI. No overlapping occurred between Fluoro-Ruby PFC injection sites. Fluoro-Ruby injection sites were observed in PL, Frontal Association (FrA), VO, VLO and DLO anteriorly and in PL, Cg1, IL, MO,VO, VLO, LO, AI, DI and GI posteriorly (Figure 1ii, iv).

Anterior PFC: There was some overlap seen between the Fluoro-Gold injection sites in PL (R28) and VO (R24). There was some minimal overlap between the Fluoro-Gold injections into VO/MO and VLO (R24 and R17). The dorsal medial Fluoro-Gold injection occurred primarily within PL (with a lesser presence in MO and VO) and the ventral medial injection occurred within VO and also MO and PL (R28 and R24). The more central injection was primarily located within VLO. The most lateral Fluoro-Gold injection occurred within DLO_2, but also occupied parts of DLO_1 and LO. Fluoro-Ruby injection sites into anterior PFC were observed in similar regions to the equivalent Fluoro-Gold injection sites, the spread of Fluoro-Ruby injections was consistently contained within the boundary of Fluoro-Gold counterparts. The dorsal medial Fluoro-Ruby injection occurred within PL and the ventral medial injection occurred within VO (R32 and R21). The more central injection was primarily located within VLO with spread into FrA, and the most lateral Fluoro-Ruby injection was primarily located within DLO_2, with some overlap into DLO_1. The Fluoro-Gold injections were typically more tear-drop shaped than the Fluoro-Ruby injections, i.e. their horizontal spread was greater. In addition to the single injections, dual injections of tracer (Fluoro-Gold and Fluoro-Ruby) were deposited at the same lower medial and lateral injection sites. The position and spread of these tracers closely

266   matched those of the corresponding Fluoro-Gold single injections (see also Figure 1i). In subsequent

267   figures these injections are referred to PL, VO, VLO and DLO (or abitarily denoted Aa, Ba, Ca and

268   Da) because the primary site of these injections was in the targeted site.

269

270   *Posterior PFC:* The dorsal medial Fluoro-Gold injection into PL (R27) spread across layers II-VI

271   and overlapped slightly with the injections targeting VO and VLO (R22 and R11). This injection

272   occupied PL, Cg1 and M2. The ventral medial injection targeting VO (R22) overlapped with the PL

273   injection (R27) and spread into IL and PL, however the majority of injected tracer was seen within

274   the intended regions of VO and MO. The central orbital, VLO injection site also spread beyond the

275   intended region (into M2), however the majority of injected tracer remained within the boundaries of

276   VLO and covered layers I-VI (R11). The lateral injection site did not overlap with any other Fluoro-

277   Gold injection sites, and was centered within the cytoarchitectural region of LO and AI (with some

278   spread into DI and GI) (R26). All of the Fluoro-Ruby injection sites produced a smaller spread of

279   tracer than the corresponding Fluoro-Gold injection sites. The dorsal medial Fluoro-Ruby injection

280   occupied both PL and Cg1 and the ventral medial injection was located within MO, IL and PL (R28

281   and R26). The central orbital Fluoro-Ruby injection was located in VLO (R25) and the lateral orbital

282   injection was in DLO_2 and DLO_1 (R27). Additional dual injections of tracer (Fluoro-Gold and Fluoro-

283   Ruby) were deposited at the same ventral medial and lateral injection sites. The spread of these tracers

284   closely resembled the equivalent Fluoro-Gold single injections but was slightly more extensive in the

285   case of the ventral medial injection (as far as just inside VLO) and (Figure 1ii).

286

287   *Afferent/Efferent labelling following PFC tracer injections*

288

289   Fluoro-Gold afferents, resultant from tracer injections into anterior (+4.7mm from Bregma) PFC were

290   found in regions of PRh (36v, 36d, 35d), Ent, AuV, Cg1, M2, M1, S1J and prefrontal regions (Figure

291   2i, Figure 3i). Fluoro-Ruby efferents resultant from tracer injections into the same co-ordinates in

292   anterior PFC were found in regions of PRh (36v, 36d, 35d), Ent, Cg1, M2 and M1, as well as

293   prefrontal regions (Figure 2iv, Figure 3iv).

294

295   Fluoro-Gold afferents, resultant from injections into posterior (+3.7mm from Bregma) PFC were

296   found in regions of PRh (35v, 35d, 36v, 36d), Ent, AuV, Cg1, M2, M1, S1J and prefrontal regions

297   (Figure 2ii, Figure 3ii). Fluoro-Ruby axon terminals resultant from injections into posterior PFC were

298   found in regions of PRh (35d, 36v, 36d), Ent, Cg1, M2 and M1, as well as prefrontal regions (Figure

299   2iv, Figure 3iv).

300

301   We also wanted to verify the location of the peri-cellular labelling of Fluoro-Ruby within the

302   projection fields. Immunofluorescent imaging of alpha-tubulin alongside Fluoro-Ruby labelling in

303   temporal cortex indicated that the majority (70%) of Fluoro-Ruby labelling we observed in temporal

304   cortex, as a result of injections into prefrontal cortex, was separate from the fluorescein labelled (i.e.

305   alpha-tubulin stained), cell bodies (Figure 4). There was some evidence of double labelling of alpha

306   tubulin and Fluoro-Ruby (Figure 4), approximately 30% of cases were found to have retrograde

307   properties (i.e. Fluorescein and Fluoro-Ruby labelling were seen in the same location).

308

309   *Organisation and distribution of connections from Anterior PFC to Temporal Cortex*

310

311   The distribution of retrograde labelled neurons in temporal cortex maintained a topology in terms of

312   the corresponding Fluoro-Gold anterior PFC injection site. Moving from medial to lateral in PFC

313   (from MO/VO to DLO), projections were seen more posteriorly within temporal cortex (fig 5i).

314

315   The distribution of anterograde efferents (from Fluoro-Ruby) in temporal cortex resultant from

316   anterior PFC tracer injections was less widespread than the corresponding retrograde afferents (from

317   Fluoro-Gold) (Figure 5iii). The distribution and topology of Fluoro-Ruby connections also differed

318   to the distribution of Fluoro-Gold projections. Although the labelling appeared in the same extent of

319   temporal cortex the Fluoro-Ruby injections produced orbital projections (moving medial to lateral,

320   MO/VO-DLO) at broadly progressively anterior locations within temporal cortex. The clearest

321   differences in the locations of anterograde and retrograde labelling resulted from injections into both

322   VO and DLO.

323

324   The distribution of anterior prelimbic projections to temporal cortex did not appear to follow a

325   topology consistent with the other orbital PFC sites: i.e. with retrograde labels in temporal cortex

326   becoming more ventrally and posteriorly positioned as injection sites in PFC moved from medial to

327   lateral; and with anterograde labels becoming more anteriorly located as injection sites in PFC moved

328   from medial to lateral. The projections arising from anterior prelimbic injections fell within this range

329   of distributions rather than outside of it. The retrograde Fluoro-Gold afferents occurred in a similar

330   temporal cortex region as the central orbital injections, i.e. VLO (Fig 5i). The anterograde, Fluoro-

331   Ruby efferents occurred in a similar temporal cortex region to the area labelled following injections

332   into the central orbital region (Fig 5iii).

333

334   Statistical analysis of the location of retrograde and anterograde projections produced the following

335   results: A two factor ANOVA (injection site [dorsal medial, ventral medial, central orbital, lateral],

336   tracer [Fluoro-Gold, Fluoro-Ruby]) revealed a significant main effect of anterior PFC injection site

337   (single and dual injections) on labelling in temporal cortex in the dorsal-ventral ($F_{(3,1200)}$=10.003

338   p<.001), anterior-posterior ($F_{(3,1200)}$=120.047 p<.001) and medial-lateral ($F_{(3,1200)}$=365.983 p<.001)

339   axes. Significant interaction effects of tracer*injection site on temporal cortex labelling were found

340   in the dorsal-ventral ($F_{(3,1200)}$=5.512 p=.001), anterior-posterior ($F_{(3,1200)}$=329.570 p<.001) and

341   medial-lateral ($F_{(3,1200)}$=204.578 p<.001) axes. The effect of injection site shows that the injection

342   position effects the location of the projections. The significant interaction reveals that the afferent

343   and efferent projections occurred at different locations over the injection sites investigated.

Organisation and distribution of Connections from Posterior PFC to Temporal Cortex

The distribution of retrograde cells within temporal cortex maintained a topological distribution according to the corresponding Fluoro-Gold posterior PFC injection sites. Moving from medial to lateral in posterior PFC (from MO/VO to AI), afferents were seen at progressively anterior locations within temporal cortex. For example, retrograde cells resultant from VO (and MO,IL,PL) injection were most posteriorly located, and VLO (and M2) injection produced labelling in more anteriorly located temporal cortex sites (fig.5ii).

The distribution of anterograde efferents maintained a topology according to Fluoro-Ruby posterior PFC injection sites which was similar to that for retrograde neurons (Figure 5iv). This was not fully the case for VO, where anterograde labelling was seen in a similar region to equivalent retrograde labelling, in addition to a more anterior location. Moving from medial to lateral in posterior PFC (MO/VO to AI), anterograde terminals in temporal cortex occurred at increasingly anterior locations (fig.5iv). In contrast to anterior PFC, injections at equivalent mediolateral injections (i.e.1.2, 2.2 or 3.3mm lateral to the midline) produced similar locations for anterograde and retrograde projections within temporal cortex.

The distribution of posterior prelimbic projections to temporal cortex also did not appear to be follow the topological organisation of the other, orbital PFC sites. The Fluoro-Gold label occurred in a relatively anterior temporal cortex location compared to the orbital injections (Fig 5ii). The anterograde, Fluoro-Ruby label again occurred in a similar temporal cortex region to the area labelled following injections into the central orbital region (Fig 5iv).

Statistical analysis of the location of retrograde and anterograde projections produced the following results: A two factor ANOVA (injection site, tracer) revealed a significant main effect of posterior PFC injection site (single and dual injections) on labelling in temporal cortex in the anterior-posterior ($F_{(3,1090)}$=394.975 p<.001) and medial-lateral ($F_{(3,1090)}$=28.494 p<.001) axes but not in the dorsal-ventral axis ($F_{(3,1090)}$=.720 p=.540). Significant interaction effects of tracer*injection site on temporal cortex labelling were found in the dorsal-ventral ($F_{(3,1090)}$=3.652 p=.012), anterior-posterior ($F_{(2,1090)}$=141.767 p<.001) and medial-lateral ($F_{(3,1090)}$=25.053 p<.001) axes.

Organisation and distribution of Connections from Anterior PFC to Sensory-motor cortex

The distribution of retrograde cells in sensory-motor cortex maintained a topology according to the corresponding (Fluoro-Gold) anterior PFC injection sites (VO, VLO and DLO). Moving from medial to lateral in PFC (from MO/VO to DLO), projections were seen more posteriorly within sensory-motor cortex (fig 6i).

The distribution of anterogradely labelled axon terminals in sensory-motor cortex maintained a different topology in terms of the corresponding Fluoro-Ruby anterior PFC injection site (Fig.6iii). Moving from medial to lateral in PFC (from MO/VO to DLO), this time projections were seen at increasingly anterior locations. For example, connections from VLO (and M2) were seen at more anterior locations compared to those arising from VO. The VO and DLO injection sites had the most different locations of anterograde efferents and retrograde afferents within sensory-motor cortex.

The distribution of anterior prelimbic projections to sensory-motor cortex did not appear to follow the topological organisation of the other orbital PFC sites. The retrograde Fluoro-Gold afferents occurred in a similar sensory-motor cortex region as the central orbital injections, i.e. VLO (Fig 6i).

394   The anterograde Fluoro-Ruby efferents again occurred in a similar sensory-motor region to the area

395   labelling following injections into the lateral orbital region, i.e. DLO (Fig 6iii).

396

397   Statistical analysis of the location of retrograde and anterograde projections produced the following

398   results: A two factor ANOVA revealed a significant main effect of anterior PFC injection site (single

399   and dual injections) on labelling in sensory-motor cortex in the dorsal-ventral ($F_{(3,1265)}$=75.39 p<.001),

400   anterior-posterior ($F_{(3,1265)}$=4.762 p=.003) and medial-lateral ($F_{(3,1265)}$=268.462 p<.001) axes.

401   Significant interaction effects of tracer*injection site on sensory-motor cortex labelling were found

402   in the dorsal-ventral ($F_{(3,1265)}$=145.429 p<.001), anterior-posterior ($F_{(3,1265)}$=116.496 p<.001) and

403   medial-lateral ($F_{(3,1265)}$=144.380 p<.001) axes.

404

405   *Organisation and distribution of connections from Posterior PFC to Sensory-motor cortex*

406

407   The distribution of retrograde cells within sensory-motor cortex maintained some topological

408   ordering according to the corresponding Fluoro-Gold injection sites in posterior PFC. Moving

409   laterally in PFC from MO/VO to AI: projections were seen more anteriorly within sensory-motor

410   cortex (fig 6ii). Here afferents from the injection into VO, MO, IL and PL (denoted Bp) and LO, AI,

411   DI and DG (denoted Dp) were located anteriorly to that resulting from injection into VO.

412

413   The distribution of anterograde, axon terminals in sensory-motor cortex maintained a topology

414   corresponding to Fluoro-Ruby posterior PFC injection sites, which resembled that of Fluoro-Gold

415   afferents. As PFC injection sites move from medial to lateral (MO/VO to AI), efferents in sensory-

416   motor cortex occurred at increasingly anterior locations (fig.6iv). In contrast to anterior PFC, the VO,

417   MO, IL and PL (denoted Bp) and LO, AI, DI and DG (denoted Dp) injection sites had similar

418   locations of anterograde and retrograde labelling within temporal cortex.

419

420   The distribution of posterior prelimbic projections to sensory-motor cortex did not appear to follow

421   a topology consistent with the other orbital PFC sites. The retrograde Fluoro-Gold afferents occurred

422   in a similar sensory-motor cortex region as the central orbital injections, i.e. VLO/M2 (Fig 6ii). The

423   anterograde, Fluoro-Ruby, efferents again occurred in a similar sensory-motor region to the area

424   labelled following injections into the lateral orbital region, i.e. injection Dp: LO, AI, DI, GI (Fig 6iv).

425

426   Statistical analysis of the location of retrograde and anterograde projections produced the following

427   results: A two factor ANOVA revealed a significant main effect of posterior PFC injection site (single

428   and dual injections) on labelling in sensory-motor cortex in the dorsal-ventral ($F_{(3,1293)}$=75.833

429   p<.001), anterior-posterior ($F_{(3,1293)}$=234.566 p<.001) and medial-lateral ($F_{(3,1293)}$=63.283 p<.001)

430   axes. Significant interaction effects of tracer*injection site on sensory-motor cortex labelling were

431   found in the dorsal-ventral ($F_{(3,1293)}$=123.547 p<.001), anterior-posterior ($F_{(3,1293)}$=4.615 p=.003) and

432   medial-lateral ($F_{(3,1293)}$=64.4 p<.001) axes.

433

434   *Results from dual injections into VO and DLO/AI*

435

436   One of the clearest results of our study was the finding that our anterior anterograde or retrograde

437   tracer injections into VO or DLO resulted in a different distribution of tracer terminations, notably

438   within the temporal cortex. To test whether this resulted from the differences in actual injections sites

439   achieved by single injections we targeted the same sites with dual injections of Fluoro-Gold and

440   Fluoro-Ruby. Fluoro-Gold and Fluoro-Ruby labelling resultant from dual tracer injections targeted

441   at anterior VO and DLO and posterior VO and AI was seen in similar regions to that observed from

442   equivalent single injections (figures 7 & 8). Furthermore, following dual injections we observed

443   essentially the same organizational pattern of connections: that injections into either anterior VO or

444   DLO resulted in FG and FR labelling in different locations. In comparison dual injections of Fluoro-

445   Gold and Fluoro-Ruby targeted at posterior VO or AI produced similar patterns of termination for

446　both the retrograde (FG) and anterograde tracer (FR). By plotting the mean location of labelling in

447　temporal and sensory-motor cortex, some differences between dual and single injections can be seen.

448　In temporal cortex, labelling from the dual injection into posterior VO (Bp) has a more lateral (i.e

449　superficial) mean location for anterograde labelling in temporal cortex than the equivalent single

450　injection (Figure 10iii). In sensory-motor cortex, retrograde labelling from the dual injection into

451　posterior VO (Bp) has a more ventral mean location (Figure 12i). The mean location of retrograde

452　labels in sensory-motor cortex has a more lateral mean location resultant from the posterior VO dual

453　injection (Bp), and for the posterior DLO (Dp) dual injection anterograde labelling has a more lateral

454　mean location ((Figure 12iii). Although the mean location of labels show these minor differences

455　between dual and single injections, the general pattern of connections remains consistent (figures 5 –

456　8). The results of these dual injections are shown in Figures 9-12 which are described below.

457

458　We plotted the location of the anterograde and retrograde tracer in three axes of orientation

459　(dorsoventral, anterior-posterior and mediolateral) within both the temporal and sensory-motor cortex

460　regions (see Figures 7-10). The graphs also include the data produced from dual injections targeted

461　at anterior VO and DLO and posterior VO and AI. The location data within temporal cortex is shown

462　following anterior (Figure 9) and posterior (Figure 10) PFC injections. The anterograde and

463　retrograde labelling shows locational differences in temporal cortex for both anterior and posterior

464　injections, however the clearest difference appears in the plotting along the anterior-posterior axis

465　following anterior PFC injections (Figure 9ii): note the difference in retrograde and anterograde

466　positions after injections denoted Ba and Da following single injections, in DLO this occurs following

467　single or dual injections. By contrast the difference in anterograde and retrograde labelling following

468　single injections into posterior PFC was much less marked in the anterior-posterior axis (Figure 10ii),

469　this result was also observed following dual injections. The distribution of anterograde and retrograde

470　tracer in the dorsoventral axis showed no obvious trends in terms of topology following anterior

471　(Fig9i) or posterior (Fig 10i) PFC injections. The distribution within the mediolateral axis following

472 anterior injections also produced no clear arrangement for anterograde or retrograde tracer (Fig 9iii).

473 However, the posterior PFC injections appear to produce a systematic shift between PFC injection

474 sites (between MO and DLO): here we observed retrograde projections occurring at increasingly

475 lateral locations within temporal cortex, i.e. superficially within cortex (Fig 10iii).

476 The location data within sensory-motor cortex following anterior and posterior PFC injections is

477 shown in figures 11 and 12 respectively and the graphs include the data produced from dual injections.

478 Again, the anterograde and retrograde labelling shows locational differences in sensory-motor cortex

479 for both anterior and posterior injections, and like the temporal cortex results, note the difference in

480 positions of anterograde efferents and retrograde afferents in the anterior-posterior axis following

481 single anterior PFC injections (Figure 11ii – injections denoted Aa, Ba and Da). Dual injections also

482 produced differences in the terminal locations for FG and FR. As was the case for the temporal cortex

483 labelling, the difference in anterograde and retrograde labelling following injections into posterior

484 PFC was less marked in the anterior-posterior axis (Figure 12ii) – this was observed following both

485 single and dual injections. The distribution of anterograde efferents in the dorsoventral axis of

486 sensory-motor cortex showed no obvious trends in terms of topology following anterior PFC

487 injections (Fig11i), however the posterior single injections of FG tracer resulted in an apparent

488 topological arrangement of retrograde terminals, with increasingly ventrally located cell bodies

489 occurring between injection sites MO and AI (Fig 12i). The distribution within the mediolateral axis

490 following anterior injections produced no clear arrangement for anterograde efferents or retrograde

491 afferents following anterior (Fig 11iii) or posterior PFC injections (Fig 12iii).

492

493 **Discussion**

494

495 Our study is the first to provide detailed analysis of how the topology of connections changes within

496 anterior and posterior portions of rat PFC. Further, we report that there are changes in the arrangement

497   of connections to both temporal and sensory motor cortices at anterior or posterior levels of rat

498   prefrontal cortex.

499

500   *Methodological and Interpretative Considerations*

501

502   Our results have shown that the FG injections produced retrograde labelling and our FR injections

503   primarily produced anterograde labelling. For FR labelling we base this judgement on the majority

504   of labelling not co-localising with alpha-tubulin (a cytosplasmic marker). We used relatively large

505   tracer injections (of 100nl FG and 100nl FR) because this produced a consistent and repeatable

506   injection volume that ensured significant labelling within the projection sites (i.e. connected regions).

507   We cannot rule out some spread to fibers of passage. The size of the tracer injections inevitably also

508   meant that tracer was not usually confined to just one sub-region of PFC, in the case of PL injections

509   there was also some spread into secondary motor cortex. In addition, our comparison of single

510   injections revealed that these were not identical in terms of mean location of projection label (figures

511   9-12) however an analysis of their distributions showed a very similar overall distribution (figures 5-

512   8). Here we aimed to look at how connectional architecture changes at anterior and posterior PFC

513   levels, however the changing shape and architecture of PFC in the A-P axis provided limitations to

514   the study (see below for a detailed discussion). It is worth also pointing out that our terms of 'anterior'

515   and 'posterior' PFC are relative, as there are significant anterior and posterior regions beyond the

516   levels we have studied (approximately 1mm anterior and approximately 2mm posterior). Therefore

517   the levels of PFC studied in this paper should both be considered to be central regions.

518

519   *Organisation of Connections from Anterior and Posterior Prefrontal Cortex to Temporal Cortex*

520

521   In this study we observed apparent topology of connections in the location of anterograde and

522   retrograde connections from both anterior and posterior PFC and to both temporal and sensory-motor

523   cortex.

524   In addition we found that for *anterior PFC* this topology of connections differed for the anterograde

525   and retrograde tracers employed. In other words, the distribution of retrograde and anterograde

526   labelling occurred in different sub-regions of temporal cortex. The differences were most notable

527   following injections into medial orbital cortex (i.e. VO) or following injections into DLO (i.e lateral

528   PFC). This is of interest because it produced a very similar topology and distribution of

529   afferents/efferents to that found following tracer injections into a 'central', coronal portion of PFC

530   (Bedwell et al, 2015), located at the equivalent coronal level of bregma +4.2mm (a coronal level half

531   way between the 2 sections in figure 1 of the present study). Specifically Fluoro-Gold and Fluoro-

532   Ruby injections into VO, VLO and DLO at this level produced afferents or efferents in

533   correspondingly similar positions within temporal and sensory-motor cortex. This study also found

534   that the distribution of anterograde and retrograde axon terminals/projecting neurons did not

535   correspond (particularly in the case of VO and DLO).

536   Further to this, we found that for the posterior PFC region we studied, the topology and distribution

537   of Fluoro-Gold (retrograde) afferents and Fluoro-Ruby (anterograde) efferents were much more

538   similar. In the case of posterior PFC; VO, MO, IL and PL (medial orbital) and LO, AI, DI and GI

539   (lateral PFC) labelled retrograde cells and anterograde axon terminals occurred in relatively similar

540   locations (in comparison to equivalent distributions following equivalent anterior medial orbital (VO)

541   and lateral orbital (DLO) injections). There could be several possible reasons for this dissociation

542   between anterior and posterior PFC. The first and most plausible reason is that the cytoarchitectural

543   regions compared are not equivalent. The most lateral injections made into the anterior PFC occupied

544   DLO, at the posterior PFC level studied the most lateral injection occupied predominantly agranular

545   insular cortex. This may explain the disparity seen in terms of different locations of retrograde

546   afferents (DLO versus AI). By examining the injection locations of the most medial orbital injections

547   (anterior versus posterior) it is also clear that, due to the changing shape of PFC subdivisions, tracer

548   occupied different subdivisons (anterior PFC: predominantly VO and MO; posterior PFC: VO, MO,

549   IL, PL). These cytoarchitectural differences in terms of injection site may help to explain the apparent

550   differences, notably in relation to the distribution of retrograde tracer. Another possible interpretation

551   for these differences is that there is a broad organisational difference within rat prefrontal cortex,

552   where anterior and central regions of PFC contain many non-reciprocal connections and posterior

553   PFC connections are more reciprocal in nature.

554   *Organisation of Connections from Anterior and Posterior Prefrontal Cortex to the Sensory-Motor*

555   *Cortex*

556   We observed strong connections between prefrontal cortex and the sensory-motor cortex. A previous

557   study has reported connections between rat orbital cortex and the cingulate cortex and secondary

558   somatic sensory motor area (Reep et al., 1996). The rat precentral medial area is also known to

559   connect to somatosensory cortex (Conde et al., 1995). In primates S1 receives afferent connections

560   from premotor areas (Cerkevich et al., 2014). Projections from the sensory-motor cortex region to the

561   different PFC regions frequently arose from distinct cortical layers within somatosensory cortex, this

562   resembled a similar pattern of projections from the striatum to the medial PFC described previously

563   (Gabbott et al., 2005) and was in agreement with our previous report concerning the connections of

564   central PFC (Bedwell et al 2014). Within the two coronal levels studied here we saw a topology

565   prominent within the connections to sensory-motor cortex of the orbital region of cortex. In common

566   with the temporal cortex connections, the topology of sensory-motor cortex-PL connections did not

567   fit within the arrangement of orbital connections (again for both FG and FR afferents/efferents). A

568   similar pattern of labelling was observed in the PFC-sensory-motor connections as was seen in the

569   PFC-temporal connections. Here the topology of anterograde and retrograde connections (arising

570   from the orbital region) differed for equivalent injections in the anterior level. However at the

571   posterior coronal level the topology observed was similar for retrograde afferents and anterograde

572   efferents seen within temporal cortex. Similarly at the level of individual injection sites this meant

573   that for posterior PFC, VO, MO, IL and PL (medial orbital) and LO, AI, DI and GI (lateral PFC),

574   labelling of retrograde afferents and anterograde efferents occurred in relatively similar locations (in

575   comparison to equivalent distributions following equivalent anterior medial orbital (VO) and lateral

576   orbital (DLO) injections). The reasons for this disparity are discussed in the preceding section on

577   PFC-temporal cortex connections.

578

579   Our analysis also shows that, in general, the distributional spread of connections became more

580   widespread in the target regions following more posteriorly located PFC injections (this was

581   particularly clear in the spread of connections to sensory-motor cortex shown in figure 6). This was

582   the case for both anterograde and retrograde connections. This indicates that there was a change in

583   the organisational patterns of divergence and convergence as we move from anterior to posterior PFC.

584   This additional change in the organisation of connections could have important implications for key

585   processing characteristics within PFC circuits.

586

587

588   **Conclusions**

589

590   Clearly the organisation of cortical connections has important functional consequences in terms of

591   both physiological organisation and function. The topology and topography of cortical connections

592   to sensory cortices supports (1) the existence of both sensory and cognitive maps and (2) important

593   perceptual functions such as visual feedback (Wang et al., 2006) and attention (Tootell et al., 1982).

594   Our study is in agreement with and provides further evidence for topologically arranged projections

595   arising from and projecting to rat PFC. Additionally our results provide evidence that the anterograde

596   and retrograde connections to orbital PFC differ in terms of their relative position and that this varies

597   according to the coronal level within PFC. In general we observed that our more posteriorly placed

598   injections produced anterograde efferents and retrograde afferents in more similar cortical positions,

599   compared to the more anteriorly placed injections. It remains to be seen whether such a trend

600   continues at progressively anterior and posterior positions within PFC. However the results indicate

601   that there are changes in the relative degree of reciprocity of connections within different regions of

602   PFC and this is likely to have important consequences for cortical processing in this important brain

603   region.

604

605

606   **Acknowledgements**

607

610

611   **Data Statement**

612

613   On acceptance of this article we plan to deposit the connectional data on the University of Rostock
614   rat connectome website: http://neuroviisas.med.uni-rostock.de/connectome/index.php.

References

615   **References**
616

617   Agster KL, Burwell RD (2013) Hippocampal and subicular efferents and afferents of the perirhinal,

618   postrhinal, and entorhinal cortices of the rat. Behav Brain Res (Netherlands) 254:50-64.

619   Alvarez JA, Emory E (2006) Executive function and the frontal lobes: A meta-analytic review.

620   Neuropsychol Rev (United States) 16:17-42.

621   Arnault P, Roger M (1990) Ventral temporal cortex in the rat: Connections of secondary auditory

622   areas Te2 and Te3. J Comp Neurol (UNITED STATES) 302:110-123.

623   Aronoff R, Matyas F, Mateo C, Ciron C, Schneider B, Petersen CC (2010) Long-range connectivity

624   of mouse primary somatosensory barrel cortex. Eur J Neurosci (France) 31:2221-2233.

625   Bedwell SA, Billett EE, Crofts JJ, Tinsley CJ (2014) The topology of connections between rat

626   prefrontal, motor and sensory cortices. Front Syst Neurosci (Switzerland) 8:177.

627   Bedwell SA, Billett EE, Crofts JJ, MacDonald DM, Tinsley CJ (2015) The topology of connections

628   between rat prefrontal and temporal cortices. Front Syst Neurosci (Switzerland) 9:80.

629   Berendse HW, Galis-de Graaf Y, Groenewegen HJ (1992) Topographical organization and

630   relationship with ventral striatal compartments of prefrontal corticostriatal projections in the rat. J

631   Comp Neurol (UNITED STATES) 316:314-347.

632   Burwell RD, Witter MP, Amaral DG (1995) Perirhinal and postrhinal cortices of the rat: A review

633   of the neuroanatomical literature and comparison with findings from the monkey brain.

634   Hippocampus (UNITED STATES) 5:390-408.

635   Cerkevich CM, Qi HX, Kaas JH (2014) Corticocortical projections to representations of the teeth,

636   tongue, and face in somatosensory area 3b of macaques. J Comp Neurol (United States) 522:546-

637   572.

638   Conde F, Maire-Lepoivre E, Audinat E, Crepel F (1995) Afferent connections of the medial frontal

639   cortex of the rat. II. cortical and subcortical afferents. J Comp Neurol (UNITED STATES) 352:567-

640   593.

641   Delatour B, Witter MP (2002) Projections from the parahippocampal region to the prefrontal cortex

642   in the rat: Evidence of multiple pathways. Eur J Neurosci (France) 15:1400-1407.

643   Frysztak RJ, Neafsey EJ (1994) The effect of medial frontal cortex lesions on cardiovascular

644   conditioned emotional responses in the rat. Brain Res (NETHERLANDS) 643:181-193.

645   Fuster JM (2001) The prefrontal cortex--an update: Time is of the essence. Neuron (United States)

646   30:319-333.

647   Gabbott PL, Warner TA, Jays PR, Salway P, Busby SJ (2005) Prefrontal cortex in the rat:

648   Projections to subcortical autonomic, motor, and limbic centers. J Comp Neurol (United States)

649   492:145-177.

650   Gattass R, Nascimento-Silva S, Soares JG, Lima B, Jansen AK, Diogo AC, Farias MF, Botelho

651   MM, Mariani OS, Azzi J, Fiorani M (2005) Cortical visual areas in monkeys: Location, topography,

652   connections, columns, plasticity and cortical dynamics. Philosophical Transactions of the Royal

653   Society of London 360:709-31.

654   Goulden N, McKie S, Thomas EJ, Downey D, Juhasz G, Williams SR, Rowe JB, Deakin JF,

655   Anderson IM, Elliott R (2012) Reversed frontotemporal connectivity during emotional face

656   processing in remitted depression. Biol Psychiatry (United States) 72:604-611.

657   Henry EC, Catania KC (2006) Cortical, callosal, and thalamic connections from primary

658   somatosensory cortex in the naked mole-rat (heterocephalus glaber), with special emphasis on the

659   connectivity of the incisor representation. Anat Rec A Discov Mol Cell Evol Biol (United States)

660   288:626-645.

661   Hoover WB, Vertes RP (2011) Projections of the medial orbital and ventral orbital cortex in the rat.

662   J Comp Neurol (United States) 519:3766-3801.

663   Kim J, Ghim JW, Lee JH, Jung MW (2013) Neural correlates of interval timing in rodent prefrontal

664   cortex. J Neurosci (United States) 33:13834-13847.

665   Kolb B (1984) Functions of the frontal cortex of the rat: A comparative review. Brain Res

666   (NETHERLANDS) 320:65-98.

667   Kondo H, Witter MP (2014) Topographic organization of orbitofrontal projections to the

668   parahippocampal region in rats. J Comp Neurol (United States) 522:772-793.

669   Krettek JE, Price JL (1977) The cortical projections of the mediodorsal nucleus and adjacent

670   thalamic nuclei in the rat. J Comp Neurol (UNITED STATES) 171:157-191.

671   Narayanan NS, Laubach M (2009) Delay activity in rodent frontal cortex during a simple reaction

672   time task. J Neurophysiol (United States) 101:2859-2871.

673   Narayanan NS, Laubach M (2008) Neuronal correlates of post-error slowing in the rat dorsomedial

674   prefrontal cortex. J Neurophysiol (United States) 100:520-525.

675   Narayanan NS, Laubach M (2006) Top-down control of motor cortex ensembles by dorsomedial

676   prefrontal cortex. Neuron (United States) 52:921-931.

677   Neafsey EJ (1990) Prefrontal cortical control of the autonomic nervous system: Anatomical and

678   physiological observations. Prog Brain Res (NETHERLANDS) 85:147-65; discussion 165-6.

679   Olson CR, Musil SY (1992) Topographic organization of cortical and subcortical projections to

680   posterior cingulate cortex in the cat: Evidence for somatic, ocular, and complex subregions. The

681   Journal of Comparative Neurology 324:237-60.

682   Paxinos G, Watson C (1998) The rat brain in stereotaxic coordinates. San Diego, CA: Academic

683   Press.

684   Porter LL, White EL (1983) Afferent and efferent pathways of the vibrissal region of primary motor

685   cortex in the mouse. J Comp Neurol (UNITED STATES) 214:279-289.

686   Reep RL, Corwin JV, King V (1996) Neuronal connections of orbital cortex in rats: Topography of

687   cortical and thalamic afferents. Exp Brain Res (GERMANY) 111:215-232.

688   Schilman EA, Uylings HB, Galis-de Graaf Y, Joel D, Groenewegen HJ (2008) The orbital cortex in

689   rats topographically projects to central parts of the caudate-putamen complex. Neurosci Lett

690   (Ireland) 432:40-45.

691   Schoenbaum G, Esber GR (2010) How do you (estimate you will) like them apples? integration as a

692   defining trait of orbitofrontal function. Curr Opin Neurobiol (England) 20:205-211.

693   Schoenbaum G, Roesch M (2005) Orbitofrontal cortex, associative learning, and expectancies.

694   Neuron (United States) 47:633-636.

695   Sesack SR, Deutch AY, Roth RH, Bunney BS (1989) Topographical organization of the efferent

696   projections of the medial prefrontal cortex in the rat: An anterograde tract-tracing study with

697   phaseolus vulgaris leucoagglutinin. J Comp Neurol (UNITED STATES) 290:213-242.

698   Smith NJ, Horst NK, Liu B, Caetano MS, Laubach M (2010) Reversible inactivation of rat

699   premotor cortex impairs temporal preparation, but not inhibitory control, during simple reaction-

700   time performance. Front Integr Neurosci (Switzerland) 4:124.

701   Stalnaker TA, Cooch NK, Schoenbaum G (2015) What the orbitofrontal cortex does not do. Nat

702   Neurosci (United States) 18:620-627.

703   Taren AA, Venkatraman V, Huettel SA (2011) A parallel functional topography between medial

704   and lateral prefrontal cortex: Evidence and implications for cognitive control. J Neurosci (United

705   States) 31:5026-5031.

706   Tootell RB, Silverman MS, Switkes E, De Valois RL (1982) Deoxyglucose analysis of retinotopic

707   organization in primate striate cortex. Science (UNITED STATES) 218:902-904.

708   Van De Werd HJ, Uylings HB (2008) The rat orbital and agranular insular prefrontal cortical areas:

709   A cytoarchitectonic and chemoarchitectonic study. Brain Struct Funct (Germany) 212:387-401.

710   Vertes RP (2006) Interactions among the medial prefrontal cortex, hippocampus and midline

711   thalamus in emotional and cognitive processing in the rat. Neuroscience (United States) 142:1-20.

712   Vertes RP (2004) Differential projections of the infralimbic and prelimbic cortex in the rat. Synapse

713   (United States) 51:32-58.

714   Wang W, Jones HE, Andolina IM, Salt TE, Sillito AM (2006) Functional alignment of feedback

715   effects from visual cortex to thalamus. Nat Neurosci (United States) 9:1330-1336.

716
717
718
719
720
721
722
723
724
725
726
727
728
729
730
731
732
733
734
735
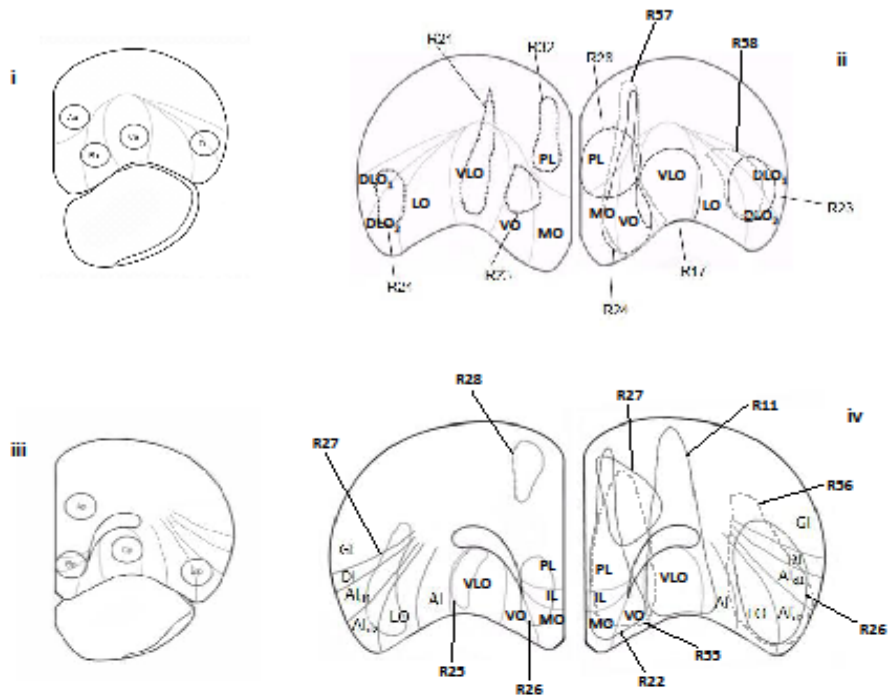
Figure 1. Tracer injections into posterior and anterior prefrontal regions. (i) Coronal section of anterior PFC (+4.7mm anterior to Bregma) showing the cytoarchitectural boundaries of PFC sub-regions according to Van de Werd & Uylings (2008), depicting sites of tracer injections; PL (Aa), VO (Ba), VLO (Ca) and DLO (Da), with 1mm separation. (ii) Representations of Fluoro-Ruby (100nl) (R21, R23, R24, R32 (broken line)) injection sites in anterior PL and FrA (R32), VO and MO (R23), VLO and FrA (R21) and DLO (R24) in the right hemisphere. Representations of Fluoro-Gold (100nl) (R17, R23, R24, R28 (solid line)) and dual Fluoro-Gold (100nl) and Fluoro-Ruby (100nl) (R57, R58 (broken grey line) injection sites in anterior PL, MO and VO (R28), VO and MO (R24, R57), VLO (R17) and DLO and LO (R23, R58) in the left hemisphere. (iii) Coronal section of posterior PFC (+3.7mm anterior to Bregma) showing the cytoarchitectural boundaries of PFC sub-regions according to Van de Werd & Uylings (2008), depicting intended sites of tracer injections; PL (Ap), VO (Bp), VLO (Cp) and AI (Dp), with 1mm separation. (iv) Representations of Fluoro-Ruby (100nl) (R25, R26, R27, R28 (broken line) injection sites in PL, Cg1 and M2 (R28), VO, MO, PL and IL (R26), VLO (R25) and AI, LO, DI and GI (R27), in the right hemisphere. Representations of Fluoro-Gold (100nl) (R11, R22, R26, R27 (solid line)) and dual Fluoro-Ruby (100nl) and Fluoro-Gold (100nl) (R55, R56 (broken grey line)) injection sites in PL, Cg1 and M2 (R27), VO, MO, PL and IL (R22, R55), VLO and M2 (R11) and LO, AI, DI and GI (R26, R56), in the left hemisphere. The diagrams represent an amalgamation of injection sites from the animals indicated by the 'R' number.

737
738
739
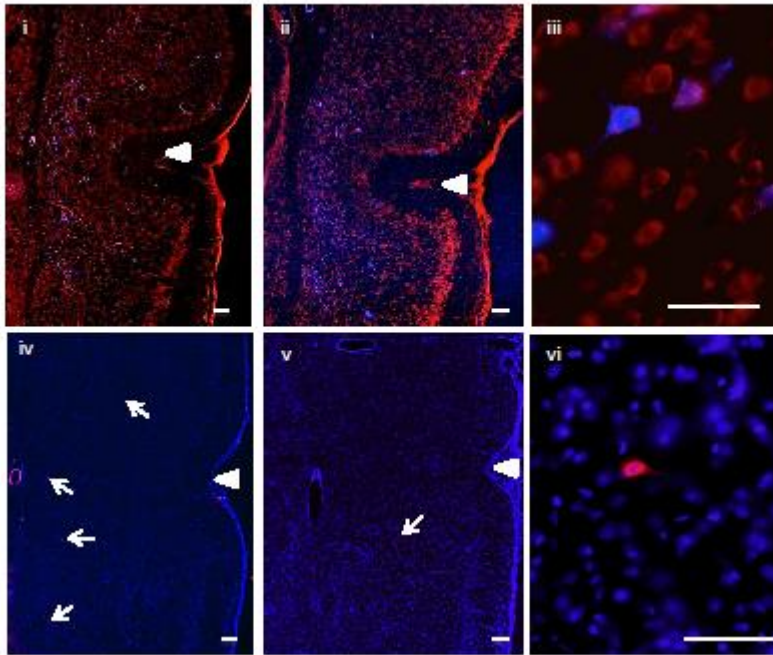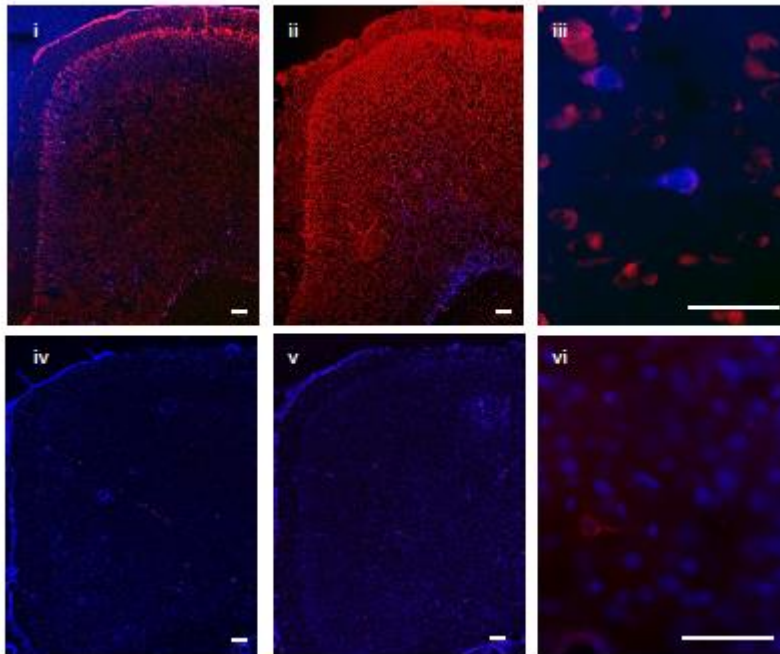740
741
742
743
744
745
746
747
748
749

Figure 2. Coronal sections showing retrogradely labelled cells (blue) in temporal cortex produced by injections of 100nl Fluoro-Gold into (i) anterior VO (R24), (ii) posterior VO (R22) (x4) and (iii) high magnification photomicrograph showing posterior PL (R27) (x20). Propidium Iodide was used to stain the background cells (red). Coronal sections showing anterograde labelling of axon terminals (red) in temporal cortex produced by 100nl Fluoro-Ruby injections into (iv) anterior VO (R23), (v) posterior VO (R26) (x4) and (vi) high magnification photomicrograph showing Fluoro-Ruby labelling from injection into posterior VLO (R25) (x20). DAPI was used to stain the background cells (blue). The triangles denote the location of the rhinal sulcus. Arrows indicate locations of Fluoro-Ruby labelling. Scale bars = 100µm.

752
753
754
755
756
757
758
759
760
761
762
763

Figure 3. Coronal sections showing retrogradely labelled cells (blue) in sensory-motor cortex produced by injections of 100nl Fluoro-Gold into **(i)** anterior VO (R24), **(ii)** posterior VO (R22) (x4) and **(iii)** high magnification photomicrograph showing anterior VO (R24) (x20). Propidium Iodide was used to stain the background cells (red). Coronal sections showing anterograde labelling (red) in temporal cortex produced by 100nl Fluoro-Ruby injections into **(iv)** anterior VO (R23) (x4), **(v)** posterior VO (R26) (x4) and **(vi)** high magnification photomicrograph showing posterior VO (R26) (x20). DAPI was used to stain the background cells (blue). Scale bars = 100µm.

767
768
769
770
771
772
773
774
775
776
777
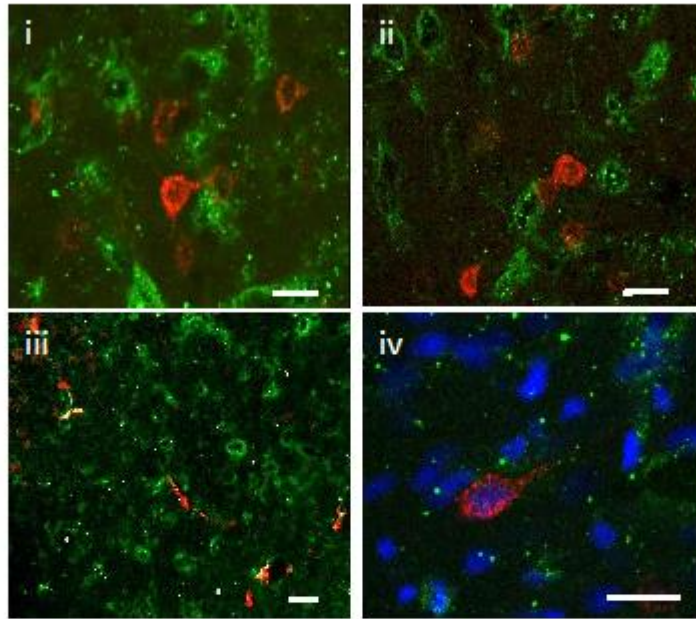
Figure 4. (i, ii & iii) Images of temporal cortex depicting fluorescently (fluorescein) labelled alpha tubulin (green) and Fluoro-Ruby labelling (red) resultant from (100nl) injection into PFC (Animal ID = R39). (iv) Image of temporal cortex depicting fluorescently labelled alpha tubulin (green), DAPI labelled nuclei (blue) and Fluoro-Ruby labelling (red) resultant from (100nl) injection into PFC. Dual-labelling of Fluoro-Ruby and Fluorescein (alpha tubulin) is shown by yellow fluorescence (iii). Scale bars = 20μm.

779
780
781
782
783
784
785
786
787
788
789
790
791
792
793
794
795
796
797
798
799
800

801
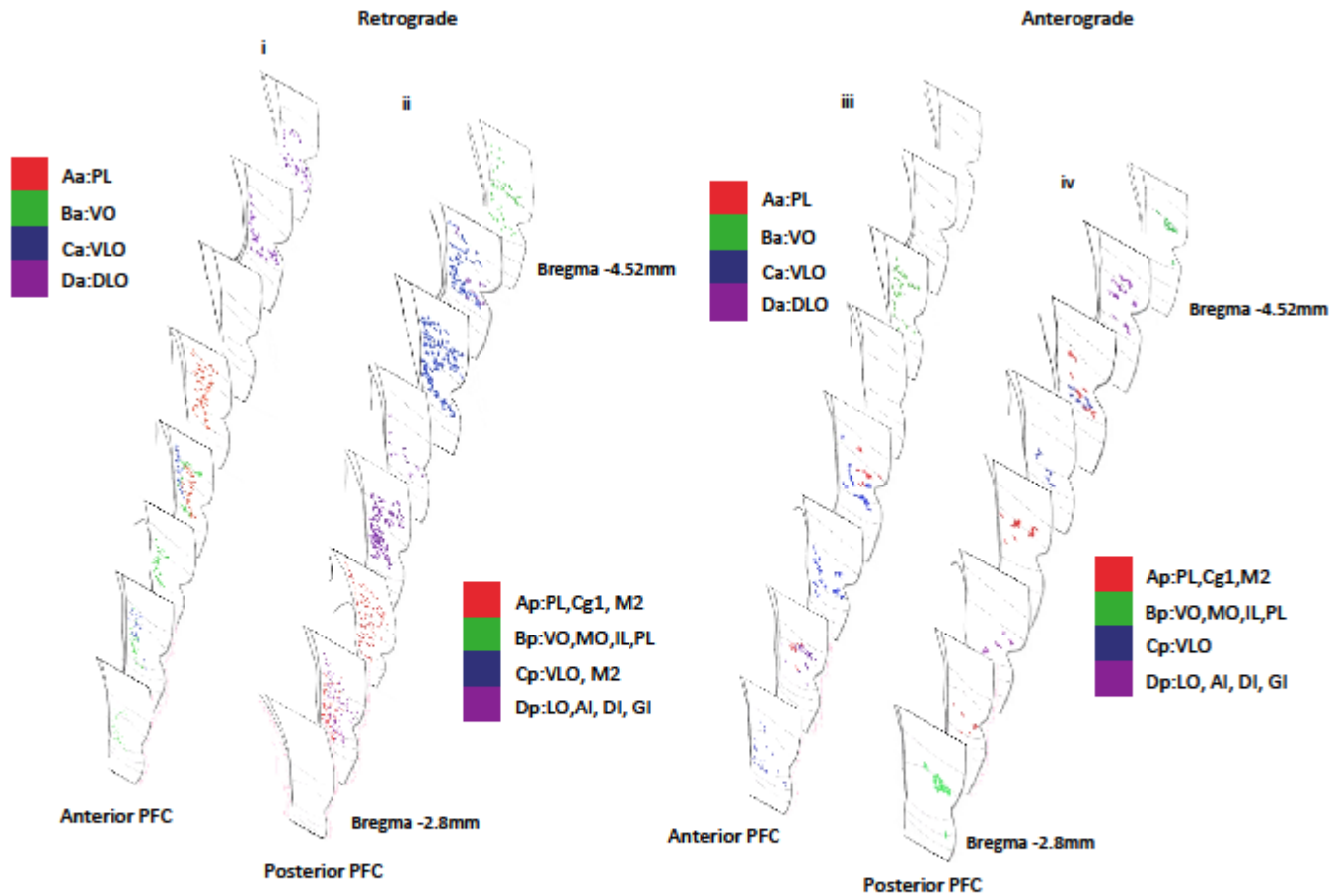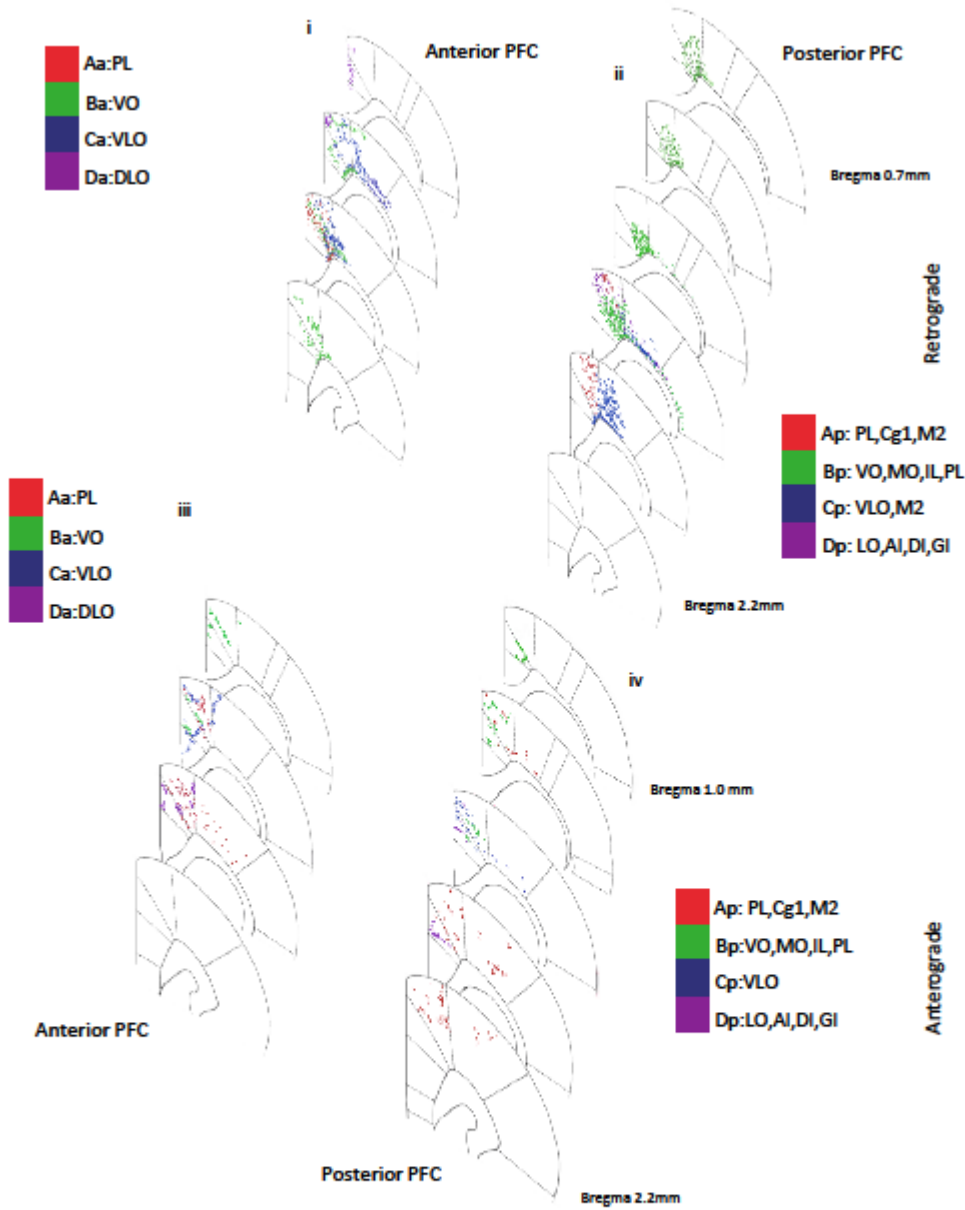

Figure 5. Diagram representing both retrograde (Fluoro-Gold) and anterograde (Fluoro-Ruby) projections to temporal cortex arising from tracer injections into the anterior and posterior PFC. (i) retrograde cells in temporal cortex produced by Fluoro-Gold (100nl) injections into anterior PFC and (ii) posterior PFC. (iii) anterograde labelling of axon terminals in temporal cortex produced by Fluoro-Ruby (100nl) injections into anterior PFC and (iv) posterior PFC. The diagrams represent an amalgamation of injection sites from the animals included in the study.

802
803
804
805
806
807
808
809
810
811
812
813
814
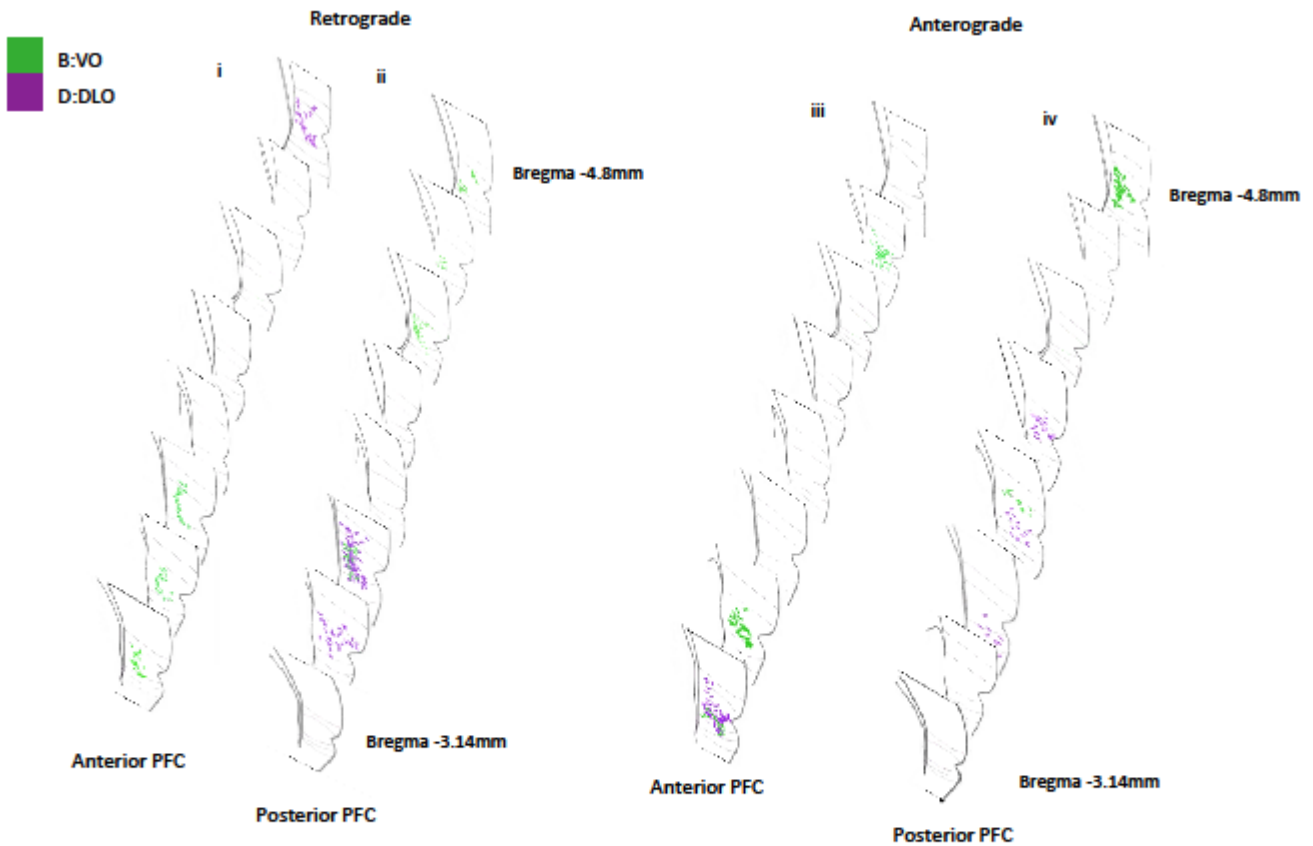815
816
817
818
819
820
821
822
823

34

Figure 6. Diagram representing both retrograde (Fluoro-Gold) and anterograde (Fluoro-Ruby) projections to sensory-motor cortex arising from tracer injections into the anterior and posterior PFC. **(i)** retrograde cell labelling in sensory-motor produced by Fluoro-Gold (100nl) injections into anterior PFC and **(ii)** posterior PFC. **(iii)** anterograde terminal labelling in sensory-motor cortex produced by Fluoro-Ruby (100nl) injections into anterior PFC and **(iv)** posterior PFC. The diagrams represent an amalgamation of injection sites from the animals included in the study.

Figure 7. Diagram representing both retrograde (Fluoro-Gold) and anterograde (Fluoro-Ruby) projections to temporal cortex arising from dual tracer injections into anterior and posterior PFC. **(i)** retrograde labelling in temporal cortex produced by Fluoro-Gold, from dual injections into anterior PFC and **(ii)** posterior PFC. **(iii)** anterograde labelling in temporal cortex produced by Fluoro-Ruby, from dual injections into anterior PFC and **(iv)** posterior PFC.

841
842
843
844
845
846
847
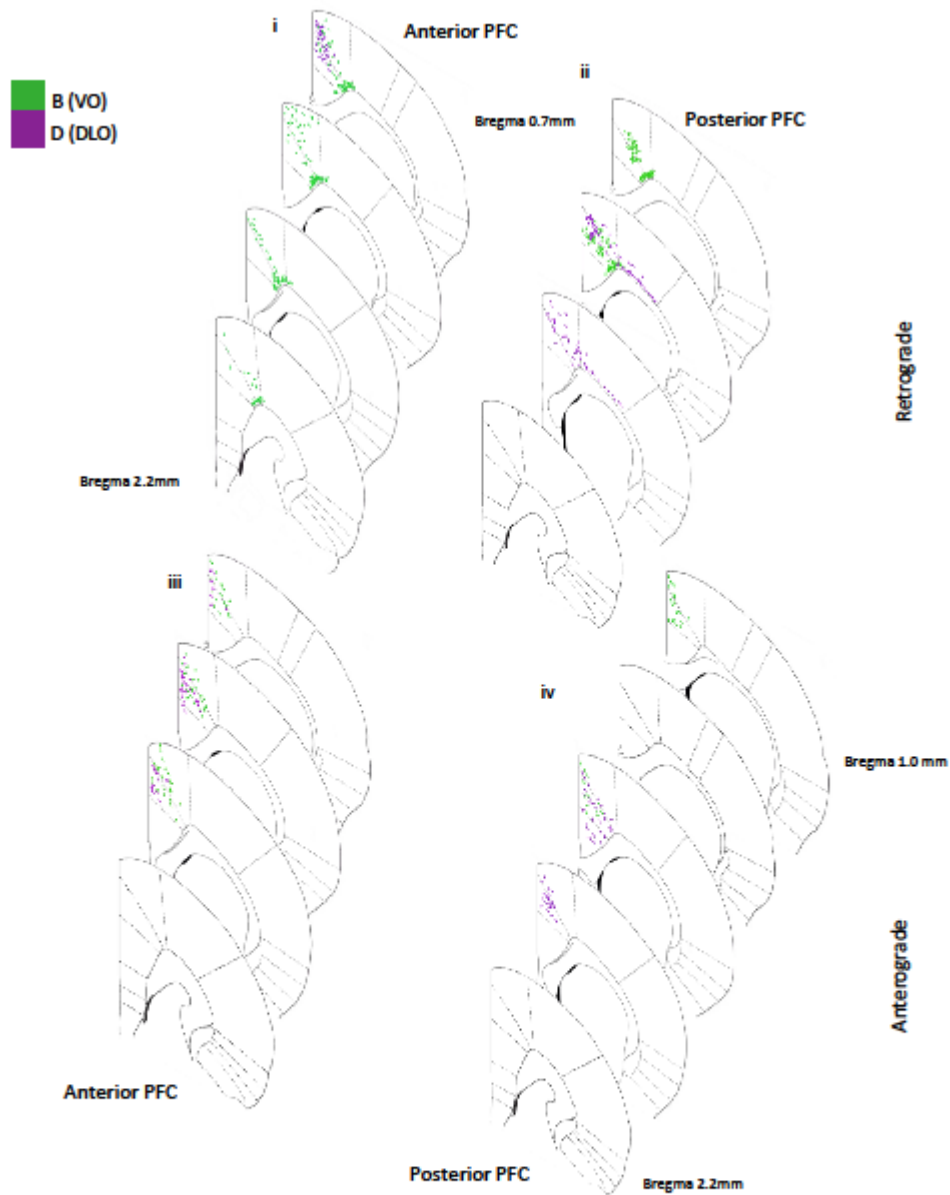848
849
850
851
852
853
854
855
856
857
858
859
860

Figure 8. Diagram representing both retrograde (Fluoro-Gold) and anterograde (Fluoro-Ruby) projections to sensory-motor cortex arising from dual tracer injections into anterior and posterior PFC. **(i)** retrograde labelling in sensory-motor produced by Fluoro-Gold, from dual injections into anterior PFC and **(ii)** posterior PFC. **(iii)** anterograde labelling in sensory-motor cortex produced by Fluoro-Ruby, from dual injections into anterior PFC and **(iv)** posterior PFC.
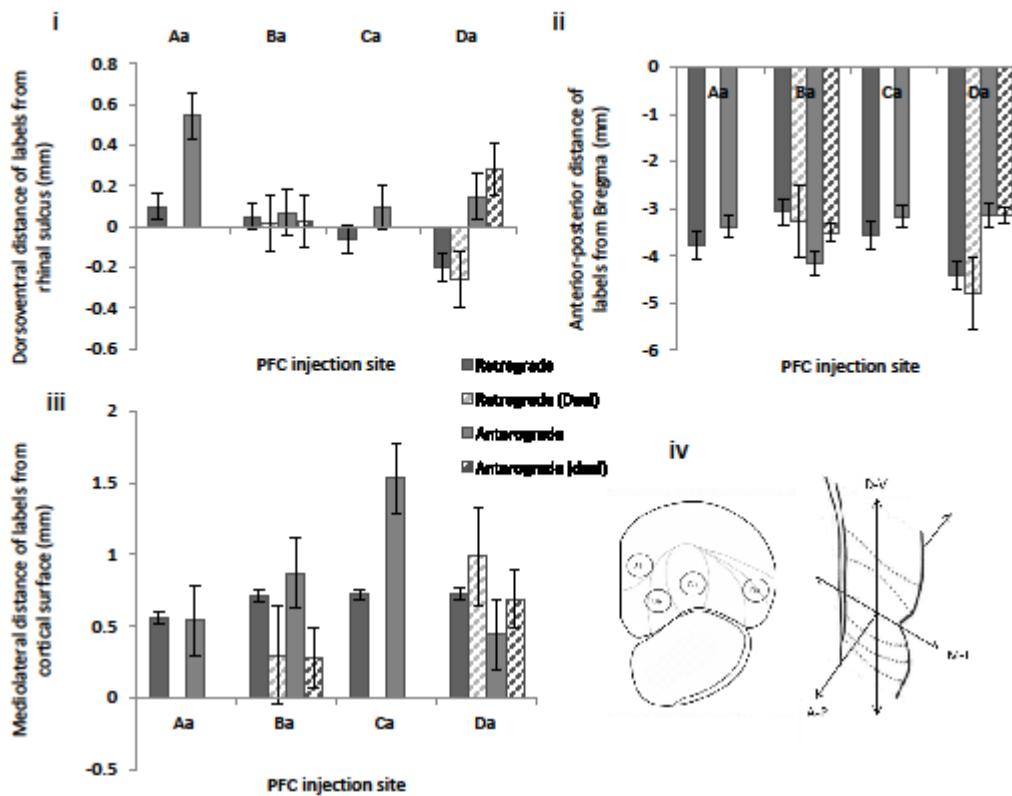
865
866
867
868
869
870
871
872
873
874

Figure 9. The mean effect of anterior PFC injection site on the location of retrograde (Aa n=75, Ba n=102 [dual injection n=157], Ca n=334, Da n=67 [dual injection n=16]) and anterograde (Aa n=47, Ba n=29 [dual injection n=224], Ca n=113, Da n=31 [dual injection n=28]) afferents and efferents in temporal cortex in (i) dorsoventral, (ii) anterior-posterior and (iii) mediolateral axes. (iv) Coronal cross section of PFC indicating the position of four injection sites within PFC: Prelimbic (injection Aa), Ventral Orbital (injection Ba), Ventrolateral Orbital (injection Ca) and Dorsal Lateral Orbital (injection Da), coronal cross section of temporal cortex, depicting the three dimensions in which the locations of labelled cells were recorded. Error bars = standard error.
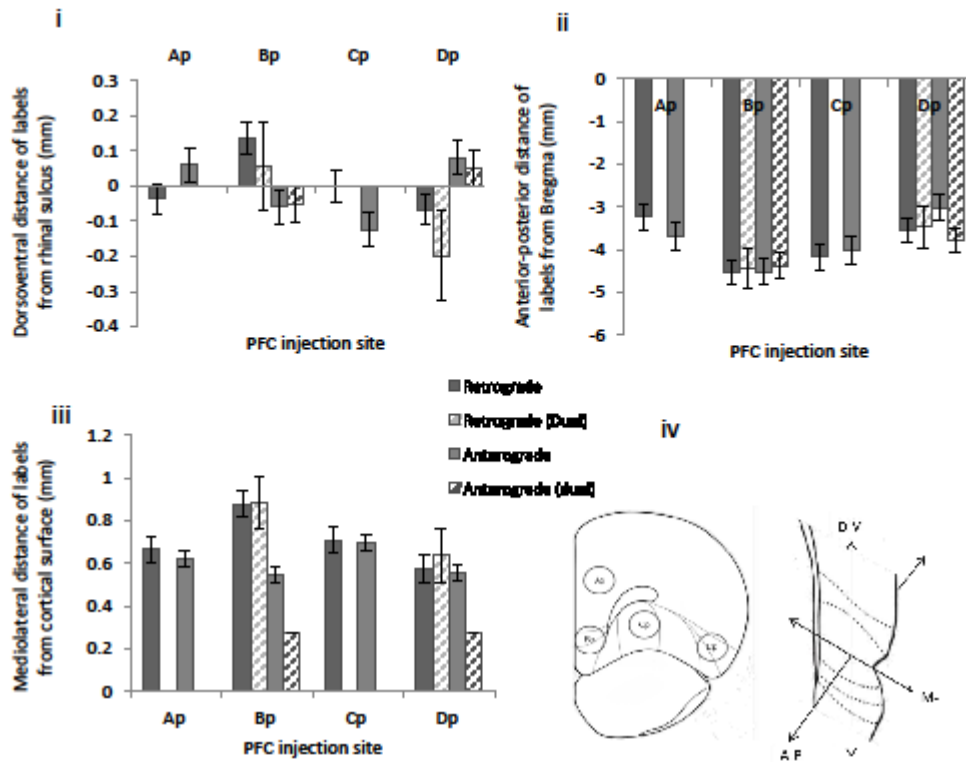
877
878
879
880
881
882
883
884
885
886
887
888

Figure 10. The mean effect of posterior PFC injection site on the location of retrograde (Ap n=114, Bp n=25 [dual injection n=159], Cp n=85, Dp n=45 [dual injection n=143]) and anterograde (Ap n=51. Bp n=36 [dual injection n=46], Cp n=113, Dp n=61 [dual injection n=213]) afferents and efferents in temporal cortex in (i) dorsoventral, (ii) anterior-posterior and (iii) mediolateral axes. (iv) Coronal cross section of PFC indicating the position of four injection sites within PFC: : PL,Cg1, M2 (injection Ap), VO,MO,IL,PL (injection Bp), VLO,M2 (injection Cp) [VLO alone in the case of the anterograde single injection] and LO,AI,DI,GI (injection Dp), coronal cross section of temporal cortex, depicting the three dimensions in which the locations of labelled cells were recorded. Error bars = standard error.

892
893
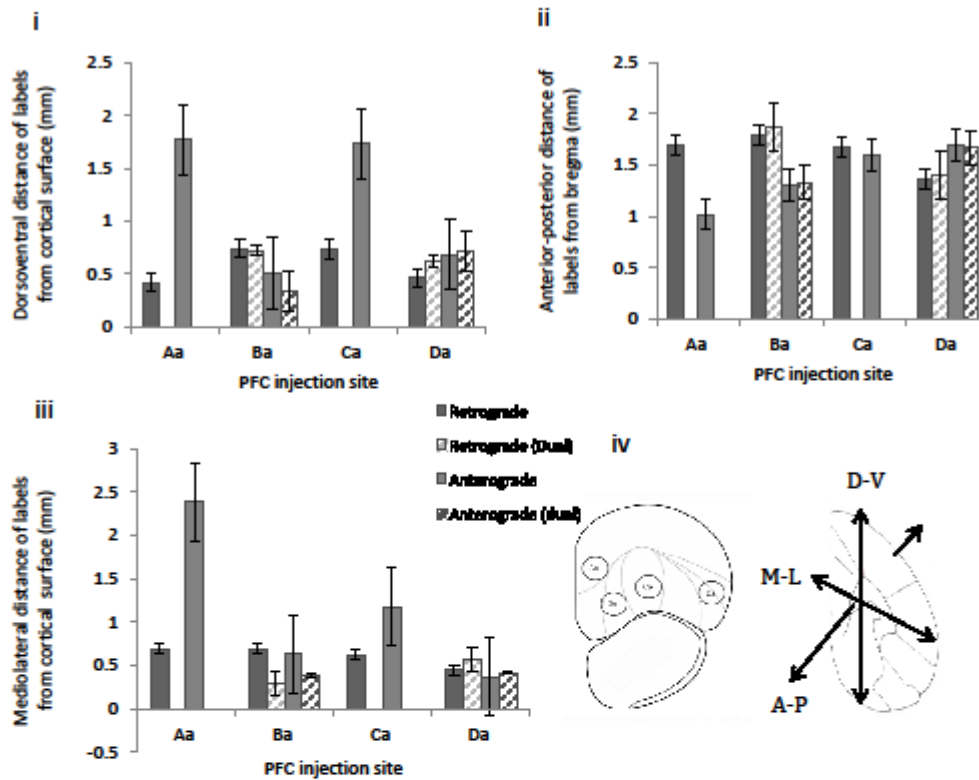894
895
896
897
898
899
900
901
902

Figure 11. The mean effect of anterior PFC injection site on the location of retrograde (Aa n=20, Ba n=77 [dual injection n=313], Ca n=39, Da n=72 [dual injection n=134]) and anterograde (Aa n=87, Ba n=91 [dual injection n=322], Ca n=30, Da n=36 [dual injection n=45]) afferents and efferents in sensory-motor cortex in (i) dorsoventral, (ii) anterior-posterior and (iii) mediolateral axes. (iv) Coronal cross section of PFC indicating the position of four injection sites within PFC: Prelimbic (injection Aa), Ventral Orbital (injection Ba), Ventrolateral Orbital (injection Ca) and Dorsal Lateral Orbital (injection Da), coronal cross section of sensory-motor cortex, depicting the three dimensions in which the locations of labelled cells were recorded. Error bars = standard error.

904
905
906
907
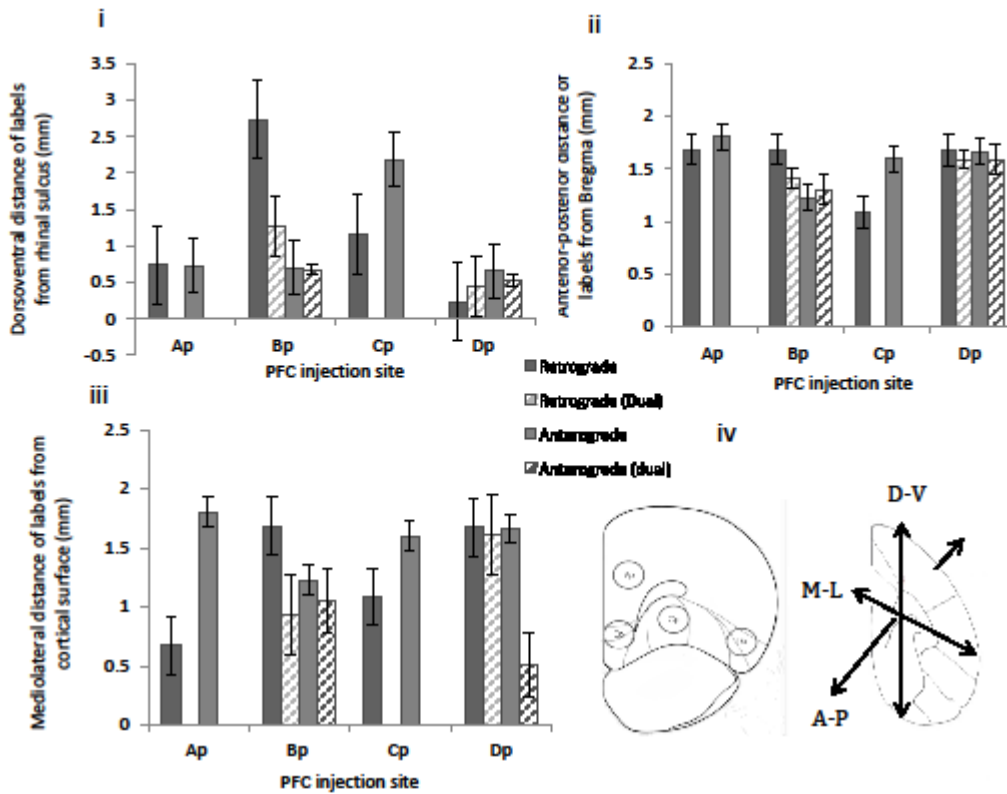908
909
910
911
912
913
914
915
916

Figure 12. The mean effect of posterior PFC injection site on the location of retrograde (Ap n=152, Bp n=268 [dual injection n=168], Cp n=136, Dp n=30 [dual injection n=227]) and anterograde (Ap n=124, Bp n=44 [dual injection n=41], Cp n=35, Dp n=40 [dual injection n=29]) afferents and efferents in sensory-motor cortex in (i) dorsoventral, (ii) anterior-posterior and (iii) mediolateral axes. (iv) Coronal cross section of PFC indicating the position of four injection sites within PFC: PL,Cg1, M2 (injection Ap), VO,MO,IL,PL (injection Bp), VLO,M2 (injection Cp) [VLO alone in the case of the anterograde single injection] and LO,AI,DI,GI (injection Dp), coronal cross section of sensory-motor cortex, depicting the three dimensions in which the locations of labelled cells were recorded. Error bars = standard error.

920
921
922
923
924
925
926
927
928
929
930

Rat ID	Hemisphere (L/R)	Tracer	AP	ML	Depth from cortical surface
11	Left	Fluoro-Gold	3.2	2.2	3.2
17	Left	Fluoro-Gold	4.2	2.2	3.2
21	Right	Fluoro-Ruby	4.2	2.2	3.2
22	Left	Fluoro-Gold	3.2	1.2	3.2
23	Right	Fluoro-Ruby	4.2	1.2	3.2
23	Left	Fluoro-Gold	4.2	3.2	3.2
24	Right	Fluoro-Ruby	4.2	3.2	3.2
24	Left	Fluoro-Gold	4.2	1.2	3.2
25	Right	Fluoro-Ruby	3.2	2.2	3.2
26	Left	Fluoro-Gold	3.2	3.2	3.2
26	Right	Fluoro-Ruby	3.2	1.2	3.2
27	Right	Fluoro-Ruby	3.2	3.2	3.2
27	Left	Fluoro-Gold	3.2	1.2	2.4
28	Left	Fluoro-Gold	4.2	1.2	2.4
28	Right	Fluoro-Ruby	3.2	1.2	2.4
32	Right	Fluoro-Ruby	4.2	1.2	2.4
37	Right	Fluoro-Ruby	4.2	2.2	1.0
38	Right	Fluoro-Ruby	4.2	3.2	1.0
39	Left	Fluoro-Ruby	3.7	1.2	3.2
55	Left	Fluoro-Ruby & Fluoro-Gold	3.2	1.2	3.2
56	Left	Fluoro-Ruby & Fluoro-Gold	3.2	3.2	3.2
57	Left	Fluoro-Ruby & Fluoro-Gold	4.2	1.2	3.2
58	Left	Fluoro-Ruby & Fluoro-Gold	4.2	3.2	3.2

Table 1. Stereotaxic location of tracer injections for each individual rat (i.e. intended locations). Stereotaxic location in terms of anterior-posterior (AP) distance with respect to bregma (these reflect the surgical stereotaxic coordinates rather than the histological coordinates confirmed later, which were slightly anterior), medial lateral (ML) distance with respect to bregma and depth from cortical surface (all in mm). The tracer type and hemisphere is also provided.

932
933
934
935
936
937